Modeling *Carcinus maenas* Settlement Patterns on the West Coast of North America

Kevin See

A thesis submitted in partial fulfillment of the requirements for the degree of

Master of Science

University of Washington

2007

Program Authorized to Offer Degree:
Quantitative Ecology and Resource Management

University of Washington
Graduate School

This is to certify that I have examined this copy of a master's thesis by

Kevin See

and have found that it is complete and satisfactory in all respects,
and that any and all revisions required by the final
examining committee have been made.

Committee Members:

_____
Jennifer Ruesink

_____
Mark Kot

Date: _____

Signature_____

Date_____

TABLE OF CONTENTS

LIST OF FIGURES

LIST OF TABLES

ACKNOWLEDGMENTS

The author would like to thank Blake Feist at the Northwest Fisheries Science Center for supporting my research. I also want to acknowledge the Pacific Marine Environmental Laboratory for providing the ROMS output which made this project possible. I would especially like to thank my wife, Virginia, and the rest of my family and friends for all of their love and support.

DEDICATION

To my grandfather, Eddie See.

Chapter 1

INDIVIDUAL-BASED MODEL

1.1 Introduction

Invasive species can cause major disruptions to local ecosystems. Currently, the rate of successful invasions by marine species in the northeast Pacific Ocean is increasing (Wonham and Carlton 2005). Identifying source populations and potential sink populations is critical for managers to effectively and efficiently allocate resources to prevent the unwanted establishment of invaders. Models of the dispersal of invasive species can help address these questions. However, modeling the spread of some marine invasive species can be difficult, primarily due to the variability of ocean transport during the planktonic larval stage (Grosholz 1996). I attempted to incorporate that spatial and temporal variability of ocean conditions by constructing an individual-based model (IBM) to simulate the spread of one recently introduced species along the west coast of North America.

The European green crab, *Carcinus maenas*, is listed as one of the world's worst invasive alien species by Invasive Species Specialist Group (Lowe et al. 2000), and it has proved to be a very successful invader worldwide. From its native range in Europe and North Africa, it has spread to the east coast of North America, southern Australia, South Africa and Japan, and it is now found on the Pacific coast of North America, from Morro Bay, California, to as far north as Vancouver Island, British Columbia (Carlton and Cohen 2003). Although green crabs utilize a variety of habitats in their native range and on the east coast of North America, their habitat on the west coast of North America is currently limited to the intertidal zone in protected estuaries (Cohen et al. 1995, Grosholz and Ruiz 1996, Jamieson et al. 1998).

Green crabs feed on a wide variety of mollusks and crustaceans, although they have

been reported to consume fish, snails and algae as well (Grosholz and Ruiz 1996, Jamieson et al. 1998, Cohen et al. 1995). They have been observed in the laboratory opening and consuming the soft-shell clam *Mya arenaria* and the mussel *Mytilus edulis* at sizes greater than the crab's carapace width (Elner 1978, Cohen et al. 1995). In addition to their varied diet preferences, they have a wide tolerance for temperature and salinity (Nagaraj 1993, deRivera et al. 2007), making the species an ideal invader. In fact, lab experiments have suggested that *C. maenas* could survive far north of its present range, as far north as Alaska (deRivera et al. 2007). Their spread is potentially aided by the length of larval duration. The planktonic larvae can take from 20 to 80 days to become competent to settle, depending on temperature (Dawirs 1985, Mohamedeen and Hartnoll 1989, Nagaraj 1993, deRivera et al. 2007).

The past and potential impacts of green crabs have been well documented in the literature. On the east coast of North America, green crabs have had a noticeable impact. Green crabs have been implicated as the cause of the decline of the soft-shell clam industry in Maine. Their arrival in the Gulf of Maine coincided with a drastic decrease in the annual catch from 1948–53 (Glude 1955). Green crabs have also been reported to negatively impact scallops, quahogs and other bivalves on the east coast (Grosholz and Ruiz 2002), and they may outcompete the native rock crab *Cancer irroratus* (Miron et al. 2005).

On the west coast, green crabs could have severe impacts on native bivalves and native crabs. Grosholz et al. (2000) found a 90–95% decline in the abundance of native clams *Nutricola tantilla* and *Nutricola confusa*, as well as the native shore crab *Hemigrapsus oregonensis*, in Bodega Bay within 3 years of the first arrival of green crabs in the bay (Grosholz et al. 2000). Green crabs learn how to crack open new shellfish prey very quickly, and they retain that knowledge for longer than other crabs from their native range (Cunningham and Hughes 1984). Lab experiments have also revealed a preference for Olympia oyster, *Ostreola conchaphila*, over several other bivalve species (Palacios and Ferraro 2003), which could impact the efforts to restore Olympia oyster populations in the Pacific Northwest. The introduction of green crabs could have negative consequences for other oyster fisheries, including those in Willapa Bay, which currently accounts for 9% of all oyster production in the United States.

There is also the potential for negative impacts upon populations of Dungeness crab, *Cancer magister*, on the west coast. Juvenile Dungeness crabs utilize the intertidal zones of estuaries as nursery grounds, bringing them into direct contact with green crabs. There is also substantial dietary overlap between juvenile Dungeness crabs and green crabs (Cohen et al. 1995, Grosholz and Ruiz 1995). McDonald et al. (2001) demonstrated that green crabs displace Dungeness crabs of equal or smaller size from refuge habitat, making the juvenile Dungeness crabs more vulnerable to predation. Green crabs could affect the Dungeness crab fishery dramatically, especially in Oregon and Washington, where green crab populations may increase substantially (Lafferty and Kuris 1996). In addition to their effects on oysters, other bivalves and native crabs, green crabs may also negatively impact shorebird populations and sentiment characteristics (Grosholz and Ruiz 2002).

The first confirmed sighting of *C. maenas* on the west coast was in San Francisco Bay in 1989. The size and circulation patterns of that bay probably led most larvae that hatched there to become entrained in the bay and settle within that estuary, promoting the growth of the population in San Francisco Bay (Cohen et al. 1995). By 1993, *C. maenas* was found in Bodega Bay, 120 km north of San Francisco (Cohen et al. 1995, Grosholz and Ruiz 1995). In 1995, several individuals were captured in Humboldt Bay (Miller 1996), 330 km north of San Francisco. The size of those crabs suggested they had arrived in Humboldt Bay in 1994. In 1997, green crabs were discovered in Coos Bay, Oregon (Yamada et al. 1999), 665 km north of the original population. The strong El Niño event in the winter of 1997–98 was correlated with that year class of green crab being distributed to estuaries in Oregon, Washington and as far north as the west coast of Vancouver Island, British Columbia (Carlton and Cohen 2003). In only a decade, green crabs have spread over 1200 km north from San Francisco Bay (Figure 1.1).

Genetic testing indicated that the eastern Pacific coast population of green crabs came from the western Atlantic stock (Carlton and Cohen 2003). They were most likely brought to San Francisco in ship ballast water. Since then, the spatial and temporal pattern of sightings indicates that their dispersal north of San Francisco is most likely due to natural rather than anthropogenic causes, namely planktonic larvae drifting in ocean currents and settling in new locations (Yamada et al. 2005).

However, closer examination of the crabs found in various estuaries indicates that new larvae are not entering estuaries at a constant annual rate. Rather, in the northern extent of the green crab's range the size frequencies are dominated by specific year classes, indicating that some years were very good recruitment years while others were not (Yamada et al. 2005). Inter-annual shifts in oceanographic patterns, such as El Niño events, have been suggested as one possible mechanism that drives the success of a particular year class in reaching northern estuaries (Jamieson et al. 2002). El Niño years are characterized by stronger and more persistent northern currents along the west coast, which could be driving green crab larvae further north than in non-El Niño years.

It is unclear which of the *C. maenas* populations north of San Francisco are permanent, and whether they can endure without new recruits from an outside source population. Therefore, questions remain about which bays are feeding the northern expansion of the crabs' range, and how the spatial and temporal variability of oceanographic currents could affect the connectivity of estuaries on the west coast. Ocean currents and temperature vary spatially and temporally, which could affect where *C. maenas* larvae settle. To determine the drivers of green crab settlement patterns, I focused on several factors that are connected to the oceanographic variability. How much of the variation in green crab settlement patterns is due to how far offshore the larvae travel, the specific bay where they are released, or the month or year they are released?

I attempted to answer this question by employing an individual based larval movement and development model that incorporates spatially and temporally specific information about ocean currents and temperatures. Individual-based models are a tool that have been developed in ecology over the past several decades and can be used to explore the underlying mechanisms of how organisms interact with their environment to produce the observed patterns that emerge in the world (Grimm and Railsback 2005). Given the lack of data related to *C. maenas* larval distribution and abundance in the northeastern Pacific, the construction of an IBM is an appropriate method for testing factors contributing to the observed patterns of green crab settlement on the west coast.

1.2 Methods

Individual Based Model

The larval behavior of green crabs, especially on the west coast of North America, is not well known. Studies from the North Sea and the Mediterranean suggest that *C. maenas* larvae may migrate vertically to take advantage of tides to advect them out to sea during the first zoeal stage and back into estuaries during the megalopae stage (Queiroga 1996; 1998, Queiroga et al. 2002; 2006). However, no such studies have been carried out in the eastern Pacific, so any larval behavior introduced into the model would be conjecture. Nor have any larval surveys been conducted in the eastern Pacific to determine how far offshore green crab larvae may be found. Given the uncertainty around larval behavior and position, a conservative approach was taken in this IBM. The west coast was treated as a one-dimensional coast, and simulations were carried out at eight separate distances offshore (10, 15, 20, 25, 30, 35, 40 and 45 km). Due to available data, it was assumed larvae traveled at a depth of 10 meters. Although no larval trawl surveys have been conducted off the west coast of North America, surveys off the coast of Portugal indicate that *C. maenas* larvae are primarily found in the top of the water column (0–30 m) with older larvae found progressively lower, down to 60 m (Queiroga 1996). It was assumed that the simulated larvae maintained the same distance offshore and the same depth during their entire development. It was also assumed the larvae could reach that offshore distance immediately after being hatched, and that they could advect onshore across that distance once they were competent to settle. Although these assumptions are not a perfect approximation of the actual larval transport process, they do lead to a simple model that can be used to analyze some of the general patterns in green crab settlement patterns.

Larval movement and development were simulated by incorporating ocean currents and temperature into an individual-based model. The ocean environment in this IBM was constructed using output from the Regional Ocean Model System (ROMS). ROMS is a physical oceanography model that is frequently used in the scientific community (Hermann and Musgrave 2006). For this study, ROMS output of ocean temperatures and northern velocity vectors from January 1997 until June 2003 was obtained (NOAA 2006). This output

was provided in time-steps of three days, on an approximately 10×10 km grid.

The simulated larvae were affected by two separate processes: ocean temperature regulated their development, and the northern velocity vector regulated their position. The larvae were treated as passive particles that drifted with the current. Both Dawirs (1985) and deRivera et al. (2007) have performed laboratory experiments to determine growth curves of the various larval stages of *C. maenas* based on temperature. I used the results presented in deRivera et al. (2007) for several reasons. First, deRivera et al. (2007) used larvae that were obtained in California, as opposed to the North Sea in Europe. Second, the predictions of larval duration were greater using the equations in deRivera et al. (2007) for temperatures greater than 11 °C, which corresponded to the majority of the ROMS output, providing a more conservative estimate of advection. The greater the larval duration, the longer the larvae are exposed to the ocean currents and further they could potentially be advected. The equations from deRivera et al. (2007) (Table 1.1) were used to compute a percentage of development for each time-step, based on the temperature at the larvaes present location. Once the larvae had completed development, they were forced by the model to settle at that latitude.

A new cohort of simulated larvae was released from the latitude of a particular bay (e.g., San Francisco Bay) at each time-step of the ROMS output, which was every three days. The northern velocity and temperature for each cohort of larvae at each time-step were determined by a weighted average of the two ROMS output points closest to the larvae's present latitude. The northern velocity determined their movement for the next three days, and the temperature determined the percentage of development that occurred over that same time period. Once each cohort of larvae had completed megalopae development, the latitude at that point was recorded as that cohort's settlement location. Cohorts were tracked by release dates, so development time and settlement locations could be attributed to specific release dates.

Similar larval transport models have been employed by Polovina et al. (1999), Kobayashi and Polovina (2006) and Kobayashi (2006). However, these previous models did not account for temperature-dependent development; they assumed a specific larval duration for all simulated larvae. In another approach, Rooper et al. (2006) averaged temperature over a 60-

day period to compute larval duration for English sole, and extrapolated alongshore currents based on three current meters off the Oregon and Washington coast. The model employed in this study utilized temperature and velocity information at a much finer resolution, thereby providing more precise results.

Statistical Analysis

The results of the IBM were combined into one database where the ultimate dependent variable was the distance larvae were advected north. The variation of this variable was explored using an ANOVA to determine how much of the variation was due to offshore distance, starting latitude, month or year released. There were eight possible offshore distances and three possible starting latitudes corresponding to San Francisco Bay, Bodega Bay and Humboldt Bay, all in California. *C. maenas* had been found in all of those bays prior to 1997. Bays further north were excluded from this analysis, due to the northern limits of the available ROMS data.

The maximum distance larvae were advected from each bay was analyzed. A linear model was fit that assumed the distance advected north was dependent on the offshore distance, starting estuary, month released and year released, as well as all two-way interaction terms. Higher-level interaction terms were omitted because of the difficulty in interpreting them biologically. An ANOVA was then performed to determine what percentage of the variation in distance advected was attributed to each of those factors, including the interaction terms. The percent contribution of variance was based on the sum of squares for each term compared to the overall total sum of squares. Although this IBM is deterministic, and therefore it is possible to explain all of the variance in this linear model by including a term for day released in the model, the smallest timeframe I was concerned with is one month. Therefore, the daily variation in ocean conditions over the course of a month was considered the residual variance in this analysis.

1.3 Results

The mean distance the simulated larvae were advected north, and the standard deviation of that distance, increased as the release location moved north. Larvae released from San

Francisco Bay were advected an average of 3.45 km (SD = 63.15), compared with an average of 17.91 km (SD = 107.01) for larvae released from Bodega Bay. Larvae released from Humboldt Bay were advected the furthest, with an average of 23.69 km (SD = 193.84).

The maximum distance larvae were advected north also varied quite widely by release location and year. Larvae released from San Francisco were advected up to 180 km in 1999–2000 but were sent as far as 368 km north in 1997–98. The maximum distance advected north for larvae released from Bodega Bay ranged from 270 km in 1998–99 to 527 km in 1997–98. Meanwhile, larvae released from Humboldt Bay had a maximum range of 225 km in 1998–99, but were advected up to 691 km in 2002–03 (Table 1.2). It is important to note that 1997–98 and 2002–03 were El Niño years, and larvae were advected much further north in those years.

The ANOVA performed on the results of the linear model showed all terms were significant to the $\alpha = 0.05$ level. Over the seven-year time-period that the IBM was run, over 6,000 cohorts of larvae were released from each of the three starting locations. With so many simulations, I expected each term to be significant. However, many of these terms did not contribute much to the overall variance. The top contributors to overall variance were "Month", "Month×Release Location" and "Month×Year". Other than those three, no other term contributed more than 5% to the overall variance (Table 1.3).

Looking at the simulated settlement locations for the three release locations and several offshore distances, a few patterns emerge. First, the offshore distance at which larvae travel does not appear to have much impact on the settlement patterns. However, the release location does make a difference. Larvae released from San Francisco tended to settle close to San Francisco, while those released from Humboldt Bay spread and settled over a much wider range. Larvae from San Francisco failed to reach the border between California and Oregon (42° N), while larvae from Humboldt Bay were advected as far north as Grays Harbor, Washington. The patterns from Bodega Bay were somewhere between the other two bays (Figure 1.2). The pattern of spread differed much more between release locations than between offshore distances.

There are also some distinct patterns when comparing seasonal releases in different years. Larvae released in the fall (September, October and November) during El Niño years

tended to drift further north than larvae released in the fall during non-El Niño years. This pattern was even more pronounced for larvae released from Humboldt Bay compared to those released from San Francisco Bay. Larvae released in the winter months (December, January and February) spread both north and south. Again, the spread was much greater for larvae released from northern California compared to those released from central California. In particular, larvae released from Humboldt Bay during the winter in El Niño years spread hundreds of kilometers further north compared to non-El Niño years, when most of the larvae were actually advected south. Finally, larvae released in the spring (March, April and May), in both El Niño and non-El Niño years, tended to be advected south of their release location (Figure 1.3).

1.4 Discussion

The distance larvae were advected varies greatly, and depends on many factors. The most important appears to be the month in which larvae were released. This primary factor accounts for the largest percentage of variation by far, almost 30%. In addition, month is part of each of the top three factors in the ANOVA analysis (Table 1.3). The second biggest contributor to the variance is the "Month×Release Location" term (13.5%). The contribution of this term probably reflects that the seasonal variability of currents is different depending on the location along the coast. The large contribution (12.8%) of "Month×Year" points to the interannual variation in the seasonal fluctuations. For example, El Niño and La Niña events can alter the magnitude of current velocity and change the timing of shifts in current directions.

The intraannual seasonal variability is most likely due to the change in the offshore surface currents over the course of a year. In general, the California Current flows south and is strongest from the summer to early fall. From Point Conception north, the northward flowing Davidson Current is strongest during the winter (Hickey and Banas 2003). Each spring, there is an abrupt shift from the northern flowing, warm current to the southern flowing, cooler current. This shift is known as the spring transition, and has been well documented in the literature (Strub et al. 1987b;a, Hickey and Banas 2003). For the rest of the spring and summer, the currents slowly change from flowing south to flowing north.

This pattern can be seen in the ROMS output as well (see Figure 1.4).

Although these overall trends hold for the entire coast, the magnitude of the California and Davidson Currents varies over space. Generally, the strength of both currents increases as one moves north (see Figure 1.5). This phenomenon could explain the difference in settlement patterns for larvae released from San Francisco Bay compared to those released from Humboldt Bay. Similar oceanographic trends exist off the California coast compared to off the Oregon or Washington coast, but they are much smaller in magnitude, with the northern velocity hovering close to zero. This could certainly be a major reason that simulated larvae released from San Francisco tended to settle very close to San Francisco.

The variability in currents across latitude is also shown in the long-distance dispersal probabilities. Although larvae from San Francisco were rarely advected north further than 200 km (1.3% of model runs), larvae from Humboldt Bay were advected at least 200 km north somewhat regularly (19.3% of model runs). At the same time, larvae also had a greater chance of flowing far to the south if they are released from Humboldt Bay, compared to San Francisco. 0.3% of larvae released from San Francisco settled 200 km south of their starting latitude, compared with 10.2% of larvae released from Humboldt Bay.

Larval duration varied from 45 to 75 days, with the longer durations occurring in the winter months when the water is colder (see Figure 1.6). Larvae that were released anytime in January would probably be in the water during the spring transition and subject to the sudden southern currents. In many years, according to the ROMS output, the spring transition occurred in mid- to late February (see Figure 1.4). This probably explains why larvae were advected further north when released in the fall compared to the winter (Figure 1.3).

C. maenas hatch eggs on different schedules depending on temperature. In the southern end of their range in Europe and eastern North America, the first zoeal stage larvae are generally found in the water year-round, with a peak between February and April (Queiroga 1996). Towards the northern edge of their range in Maine, females are restricted to hatching eggs between June and October, the warmer months (Berrill 1982). If these patterns hold for the west coast of North America, there are implications for the future spread of green crabs. Given the longer larval duration in the winter months, larvae that are released between February and April have a greater chance of being caught in the spring transition

and advected south. However, as green crabs move north and start to release more larvae in the late summer and early fall, when the currents are starting to flow north, their spread north could accelerate.

Although the month, year and location of larval release appear to have influenced the settlement patterns of *C. maenas*, the offshore distance did not (Figure 1.2). This helps to justify treating the west coast as one-dimensional, since one would have expected to see a larger difference in the nearshore larval drifts compared to the offshore drifts if a convoluted coastline had more impact on the nearshore oceanographic conditions. Because the currents and temperatures seemed somewhat uniform from 10 to 45 km offshore, the potential effects of larvae moving on- or off-shore and finding different conditions which would impact their settlement patterns were reduced, adding further justification for these model results.

San Francisco Bay is known to have a large population of green crabs. The growth of this population, after the initial introduction, could be due to the geographical size and shape of the bay, which could allow larvae to be retained without ever reaching the open sea (Cohen et al. 1995). This IBM simulation demonstrates that even if larvae do reach the open ocean from San Francisco Bay, there is a lower probability that they will be advected a great distance, which would mean more of them return to settle in San Francisco Bay. This self-recruitment could also help explain the growing population within that bay.

The patterns that appear when comparing El Niño and non-El Niño years are quite interesting (Figure 1.3). There is widespread consensus that the 1997–98 El Niño event brought *C. maenas* larvae to the Oregon and Washington coasts, as well as to Vancouver Island (Yamada et al. 2005). The assumption has been that they came from the large source population in San Francisco Bay. However, these results imply that larvae from San Francisco did not reach the border between California and Oregon, let alone Vancouver Island, even during El Niño years. This could be a result of the ROMS output not being completely accurate in reflecting the strength of northern currents during that time period. One sign that the ROMS output may not be capturing the actual ocean conditions lies in the dates of the spring transition. The spring transition dates from ROMS (Figure 1.4) are earlier than the typical dates reported in the literature (Strub et al. 1987b;a, Hickey and Banas 2003). However, this could be because oceanographers are generally concerned

with oceanographic processes further from shore than this IBM took into account, and it is possible that the spring transition occurs earlier closer to shore. ROMS output has been used extensively in a variety of oceanographic and biological models, but many of them are concerned with areas farther offshore than the scope of this IBM. Further work comparing the ROMS output with ocean current data from buoys and drifters close to shore will help address the likelihood of this possibility.

These IBM results could also imply that the surge of green crab larvae in 1997–98 may have been fueled by adult crabs in Humboldt Bay. The first confirmed green crabs appeared in Humboldt Bay in 1994. Crabs of that year class would have been four years old in the summer and fall of 1997, near their reproductive peak and possibly capable of supplying many of the larvae that later settled in Oregon, Washington and Vancouver Island estuaries. These results also show that some of the larvae released from Humboldt Bay may settle back in the bay, so the green crab population in that bay probably expanded between 1994 and 1997. Accurate surveys of the size of the green crab population in Humboldt Bay in 1997 would help provide support for or against this possibility.

1.5 Conclusions

To examine the underlying causes of variation in recruitment patterns of *C. maenas*, an individual-based model was constructed that incorporated ROMS output at a fine spatial and temporal scale. The variability in *C. maenas* recruitment patterns on the west coast of the United States is primarily due to the monthly variability in the ocean currents. This seasonal variability is different for different bays, and during different years, which also contribute to the overall variance. The distance offshore at which the larvae drift appears to play a minimal role in their north/south advection. These results predict that the furtherest northern transport of larvae from California occurs when larvae are released from Humboldt Bay during the fall of an El Niño year.

1.6 Tables

Table 1.1: Predicted larval durations for two stages, based on temperature (T). Adapted from deRivera et al. (2007).

Stage	Equation
All four zoeal	$122.96 - 34.47 \times \ln(T)$
Megalopal	$77.76 - 21.72 \times \ln(T)$

Table 1.2: Maximum distance (km) that larvae were advected in model.

	San Francisco Bay		Bodega Bay		Humboldt Bay	
Year	Advected	Offshore	Advected	Offshore	Advected	Offshore
97-98	368.0	25	527.0	25	653.9	30
98-99	274.6	45	268.7	45	225.1	40
99-00	179.5	25	310.8	40	527.4	20
00-01	249.8	45	358.3	45	473.3	35
01-02	291.4	45	367.8	45	477.9	35
02-03	344.0	45	435.1	40	691.3	25

Table 1.3: Factors that contributed at least 3% to overall variance.

Variable	DF	Contribution to Variance
Month	11	29.6 %
Month×Release Location	22	13.5 %
Month×Year	58	12.8 %
Year	6	4.6 %
Release Location×Year	12	3.4 %
Offshore Distance×Month	11	3.0 %
Other		1.7 %
Residuals	18199	31.4 %

1.7 Figures

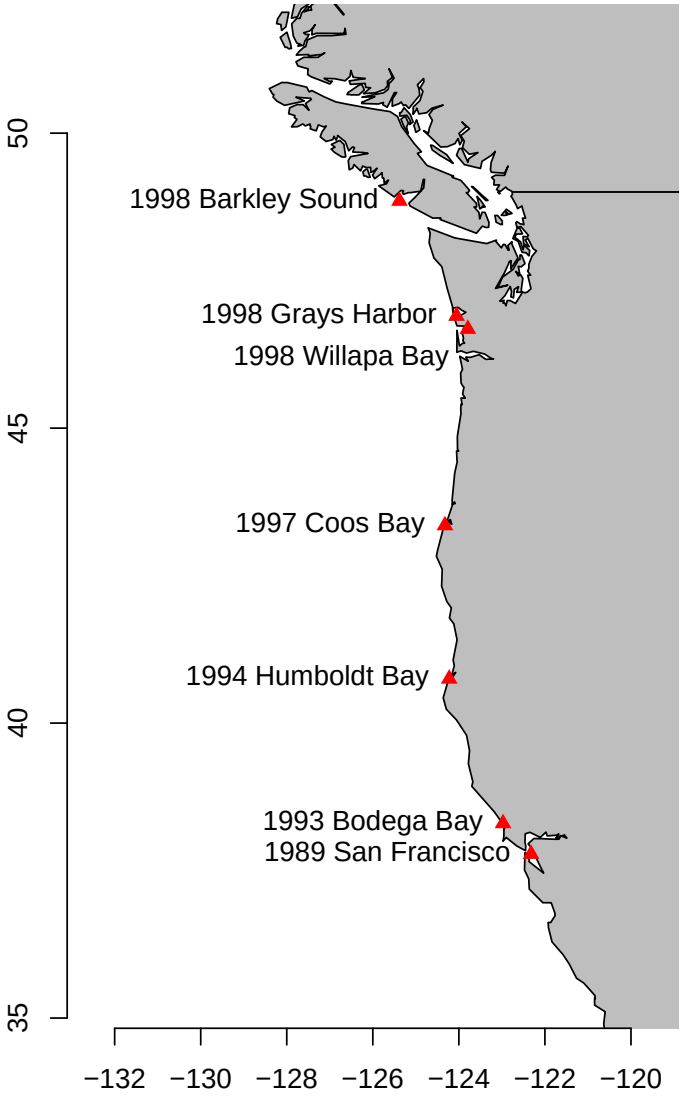

Figure 1.1: Dates of first confirmed sighting of green crabs in west coast estuaries.

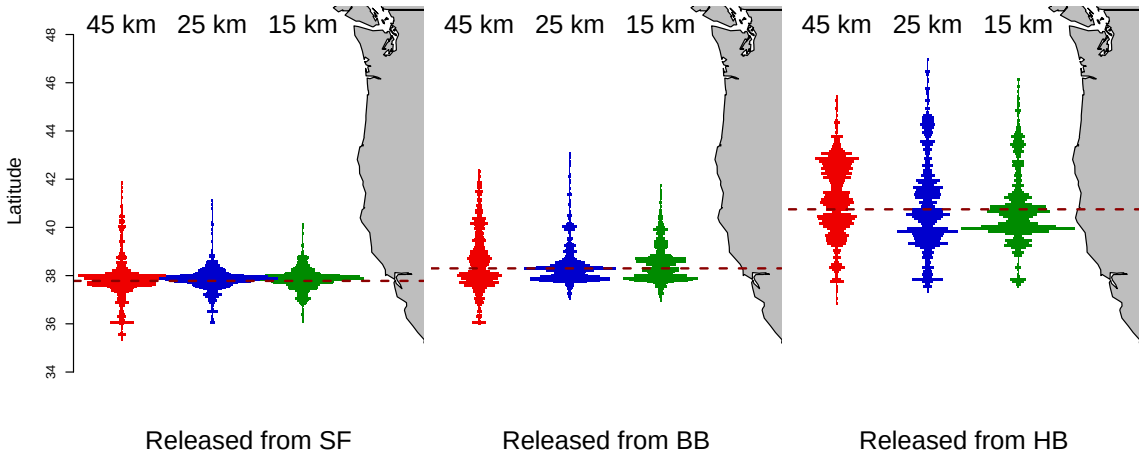

Figure 1.2: Magnitude of green crab larvae settlement for 3 release locations, and 3 offshore distances. SF=San Francisco, BB=Bodega Bay, HB=Humboldt Bay.

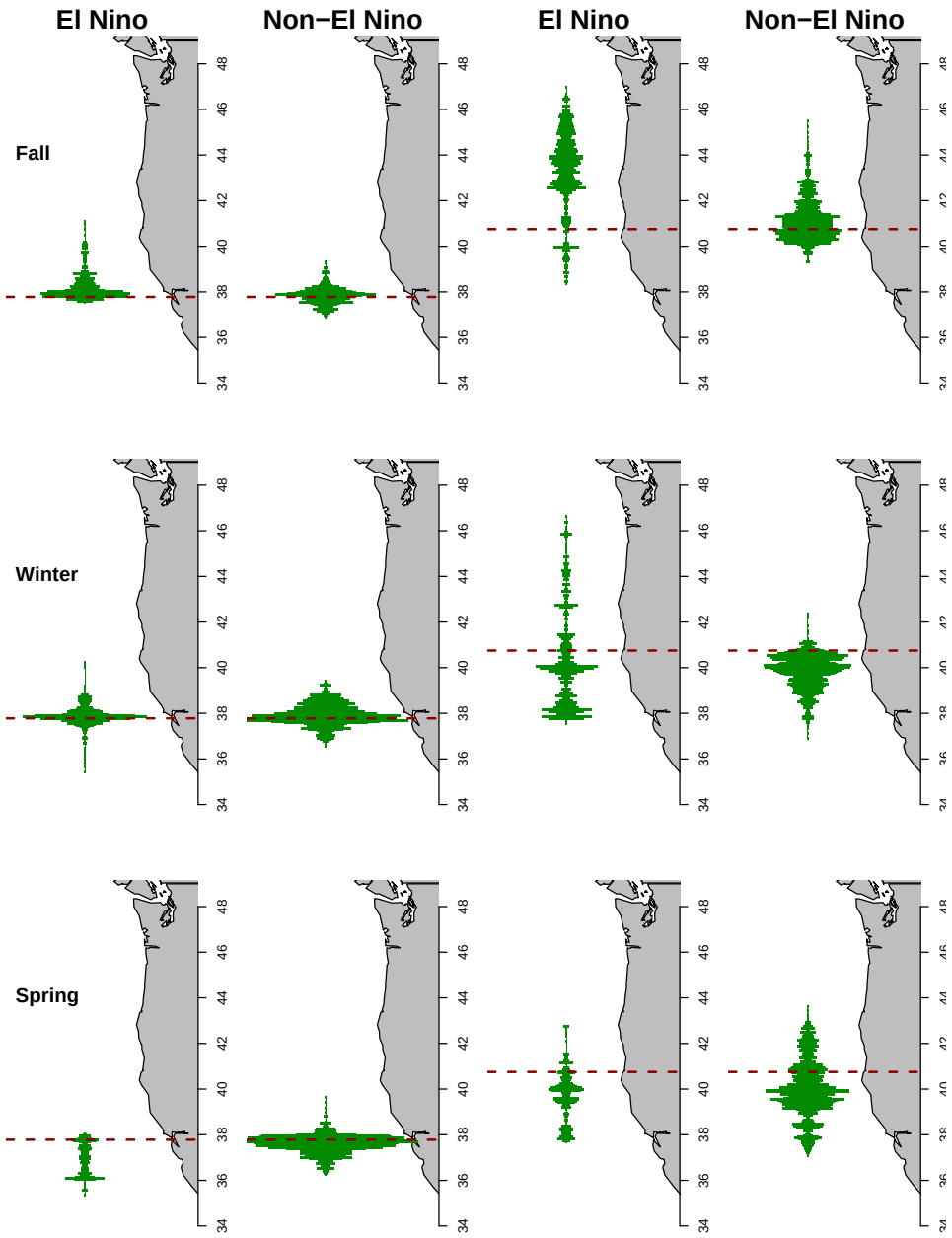

Figure 1.3: Magnitude and latitude of green crab larvae settlement for releases from San Francisco (first two columns) and Humboldt (latter two columns) bays. Further divided into season of larval release and whether released during an El Niño or non-El Niño year.

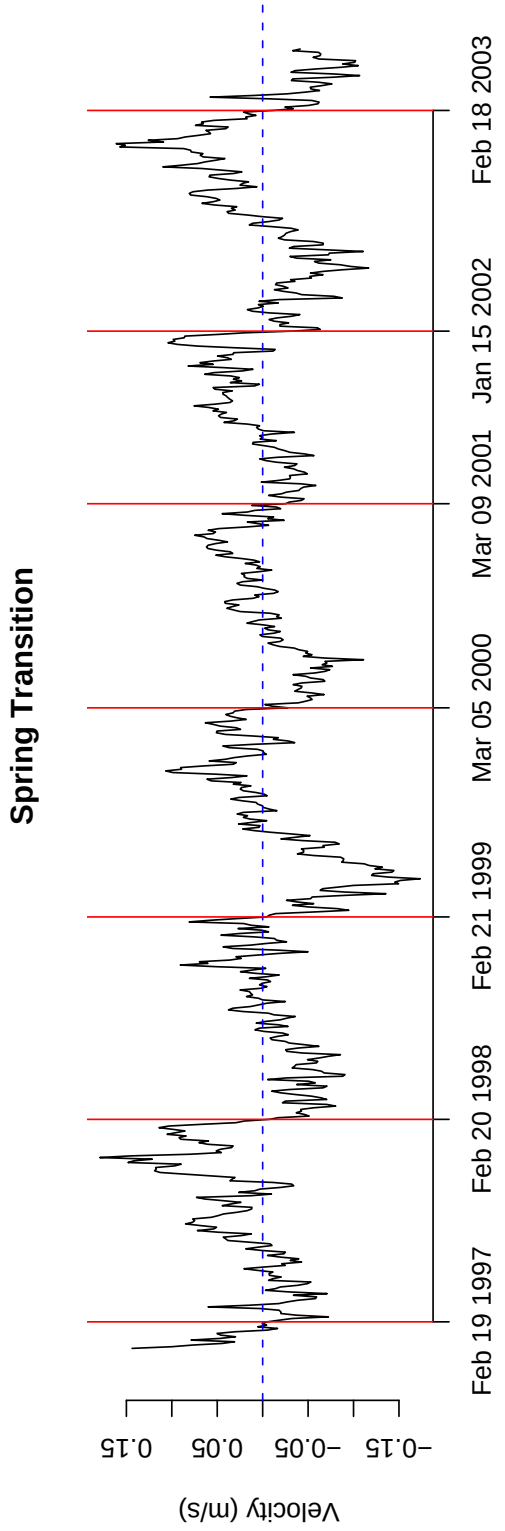

Figure 1.4: Mean northern velocity for west coast, with date of spring transition each year.

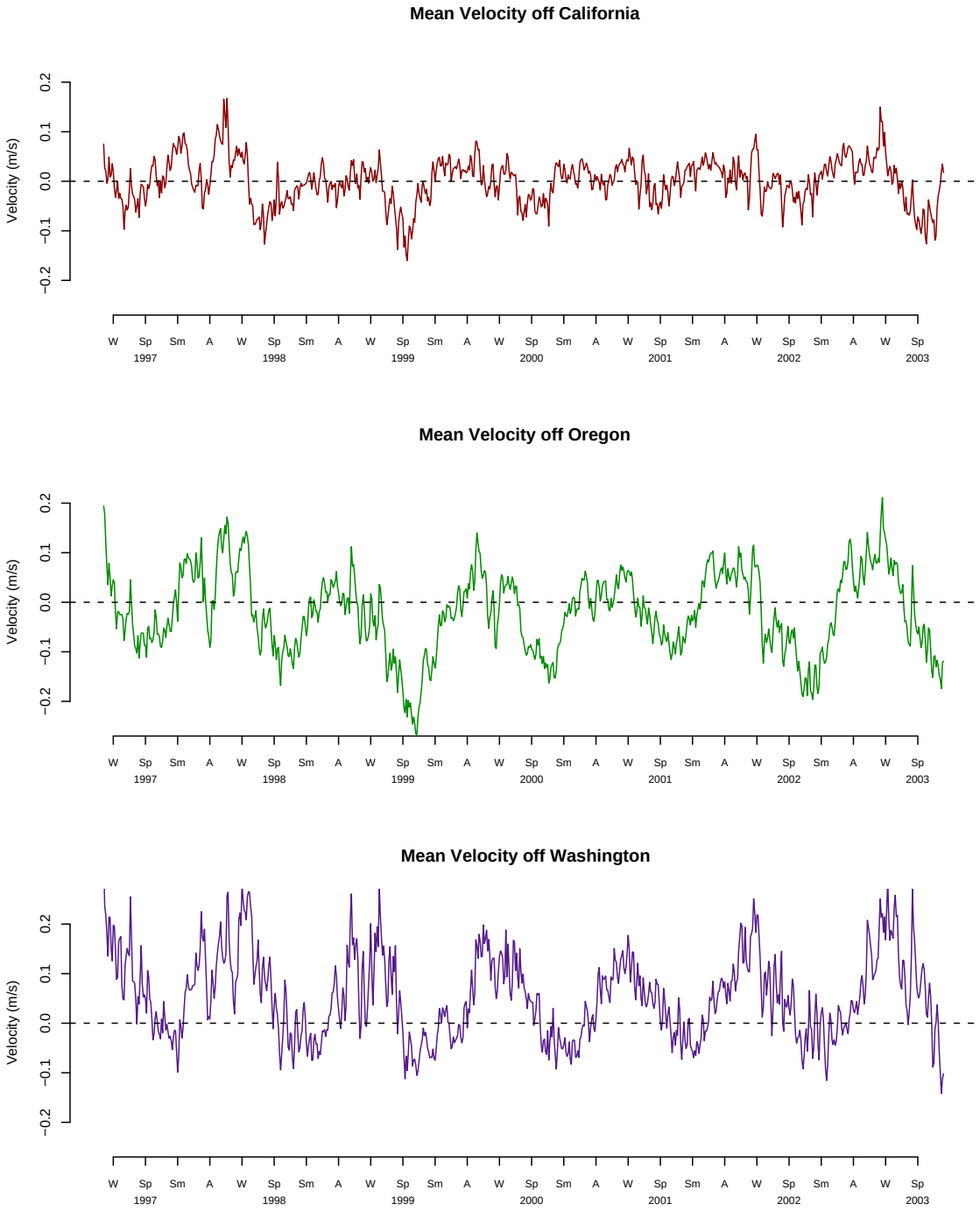

Figure 1.5: Mean velocity for each state on the west coast, computed from ROMS output.

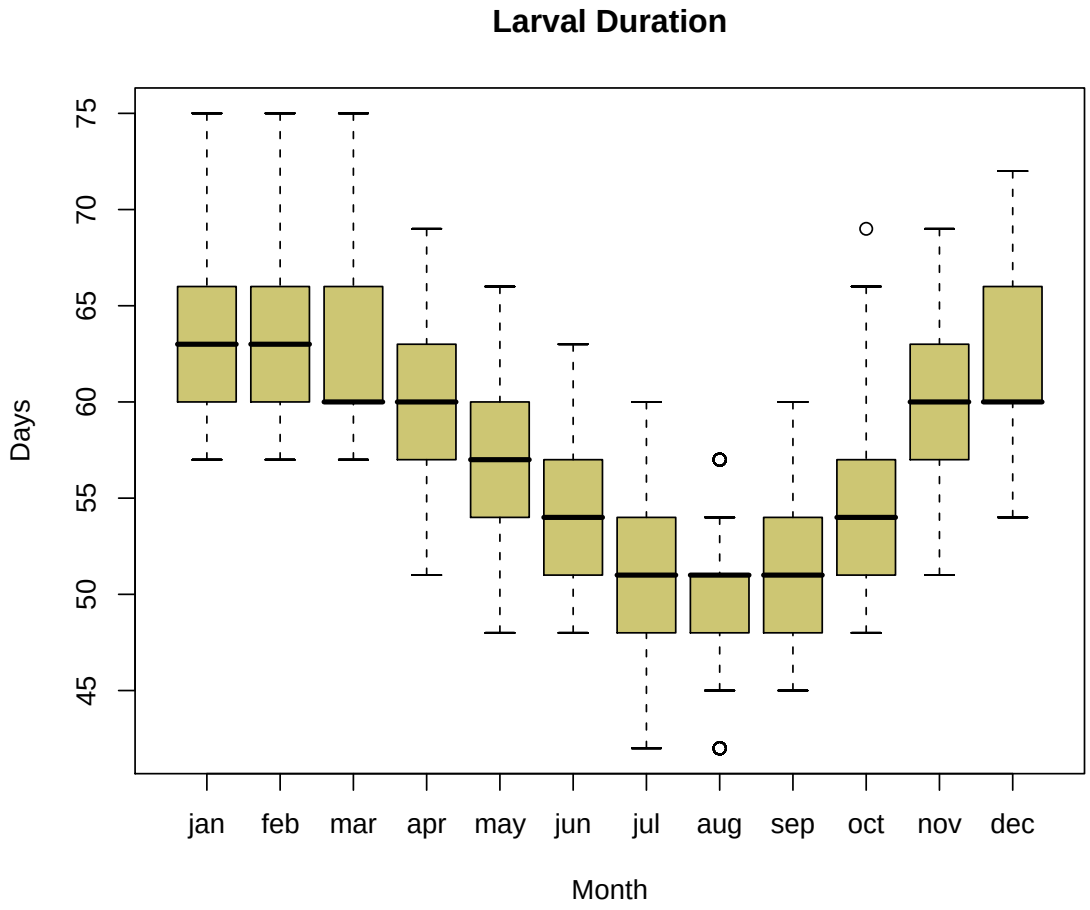

Figure 1.6: Larval durations for larvae released in each month.

Chapter 2

PARTIAL DIFFERENTIAL EQUATIONS MODEL

2.1 Introduction

Invasive species can cause major disruptions to local ecosystems. The rate of successful invasions by marine species in the northeast Pacific Ocean is increasing (Wonham and Carlton 2005). However, modeling the spread of some marine invasive species can be difficult, compared to terrestrial species, primarily due to the variability of ocean transport during the planktonic larval stage (Grosholz 1996). In this paper, I will examine one particularly successful marine invader and incorporate age structure and advection into a model of their range expansion.

The European green crab, *Carcinus maenas*, has proved to be a very successful invader worldwide. From its native range in Europe and North Africa, it has spread to the east coast of North America, southern Australia, South Africa and Japan, and it is now found on the Pacific coast of North America, from Morro Bay, California to Vancouver Island, British Columbia (Carlton and Cohen 2003). Lab experiments have suggested that *C. maenas* could survive far north of its present range, as far north as Alaska (deRivera et al. 2007). Predicting future range expansion of green crabs is critical for resource managers on the west coast of North America.

Incorporating ocean transport into marine invasion models is crucial for predicting range expansion. However, accurate data of ocean conditions are difficult to gather and most oceanographic models are extremely complex, making the output analytically intractable. Many standard reaction-diffusion or integrodifference models are inappropriate here because they fail to account for the inherent age structure of the larvae, which determines when they are functionally able to settle out of the plankton and into an estuary. To study this system, advection due to the ocean currents and the age structure of the larvae should be incorporated into a one-generation model. Therefore, an advection-based partial differential

equation model that includes age structure was created. In this paper, this model is solved, and its sensitivity of it to a number of ocean velocity functions is explored.

2.2 Natural and Invasion History of C. maenas

Green crabs prey on a variety of mollusks and crustaceans (Grosholz and Ruiz 1996) although they tend to focus on bivalves and smaller crabs. They have a wide tolerance for temperature and salinity (Nagaraj 1993, deRivera et al. 2007), making them an ideal invader. Although green crabs are found in a variety of habitats in their native range and on the east coast of North America, on the west coast they have only been trapped in the intertidal range within protected bays and estuaries. Their planktonic larvae develop in 20 to 80 days, depending on temperature (Dawirs 1985), before settling out and joining the benthos.

The first confirmed sighting on the west coast was in San Francisco Bay in 1989. The population was fairly confined there until 1993, when adult crabs were found in Bodega Bay, about 100 km north. In 1994, *C. maenas* was found in Monterey Bay and in 1995, it was found as far north as Humboldt Bay, over 300 km north of San Francisco Bay. The green crab crossed the Oregon border in 1997 when it traveled an additional 300 km from Humboldt Bay and was found in Coos Bay. From there, it spread north to various Oregon estuaries and into Willapa Bay and Gray's Harbor, Washington in 1998, 425 km north of Coos Bay. Specimens were then found on Vancouver Island, British Columbia in 1999 and 2000 (Carlton and Cohen 2003). These sighting dates indicate that the invasion of green crab has not moved at a constant rate.

Genetic testing indicated that the eastern Pacific coast population of green crabs came from the western Atlantic stock (Carlton and Cohen 2003). They were most likely brought to San Francisco in ship ballast water. Since then, the spatial and temporal pattern of sightings indicates that green crab dispersal north of San Francisco is most likely due to natural causes, namely planktonic larvae drifting in ocean currents and settling in new locations (Yamada et al. 2005).

2.3 An Advection and Age-Structured Model

I postulate that the change in the density of larvae at a particular window in space, in a particular window in time, and of a particular window of age can be modeled by assuming a conservation of larvae. The change in larval density is related to the number of larvae that move through that window and settle out of the plankton. This relationship can be expressed as

$$\bigtriangledown \rho(a,t,x) \cdot \vec{v} = -\mu_s(a)\, \rho(a,t,x), \tag{2.3.1}$$

where

$$\rho(0,t,x) = B(t,x). \tag{2.3.2}$$

In this model, a is the age of the larvae, t is a particular moment in time, and x is the distance north of an originating bay such as San Francisco. $\rho(a,t,x)$ is the density of larvae of age a, at time t in location x. $\mu_s(a)$ is a function describing the per capita settling rate at a particular age. $\vec{v}$ is a velocity vector expressing how the larvae move through age, time and space, $(v_a, v_t, v_x)^T$. The initial condition is a birth function, $B(t,x)$, describing the density of larvae of age 0 which are released at time t from location x.

This model makes several assumptions. First, I am assuming a one-dimensional coast, so the ocean currents (and therefore the larvae) only move north and south. Given the geography of the west coast, this is not an unreasonable assumption, and seems a logical place to start. This also glosses over any east/west impediments to settling, such as tidal fluctuations, river plumes, and other potential oceanographic barriers that would prevent larvae from settling anywhere along the coast.

For the velocity vector, I assume that larvae move through age and time at the same rate, so $v_a = v_t = 1$. I also assume that velocity can be described solely as a function of time, $v_x = v(t)$, and is spatially uniform up and down the coast. Based on the plots of velocities over space and time (see Figure 2.1), velocities appear more homogeneous over space than over time, so this assumption is fairly reasonable as a general approximation.

In addition, I assume that the age at which larvae are ready to settle is determined solely by time, and not by a more complicated function involving temperature or a proxy

for temperature such as latitude. This is a simplifying assumption, but seems a reasonable place to start. It could be some kind of probability distribution, so that most larvae develop at the mean development age, but there is some variation. This distribution would help capture some of the variation in development time due to temperature.

The partial differential equation model can now be expressed as

$$\frac{\partial \rho}{\partial a} + \frac{\partial \rho}{\partial t} + v(t)\frac{\partial \rho}{\partial x} = -\mu_s(a)\rho, \tag{2.3.3}$$

with the same initial condition.

To evaluate this model analytically, functions that can be integrated are needed to desribe current velocities and larval settlement. This may cause some restrictions on how these processes are described, but it may not matter if the biologically relevant patterns are captured appropriately. If these processes are described with functions that cannot be integrated analytically, the answer can be approximated numerically, which may be enough for resource managers.

To solve this equation, I apply the method of characteristics. This technique involves a change of variables, from (a, t, x) to (ξ, η, θ). To make this change of variables, I assume that

$$\frac{\partial t}{\partial \xi} = 1, \tag{2.3.4}$$

$$\frac{\partial a}{\partial \xi} = 1, \tag{2.3.5}$$

$$\frac{\partial x}{\partial \xi} = v(t). \tag{2.3.6}$$

From these assumptions, it follows that

$$\frac{\partial \rho}{\partial \xi} = -\mu_s(a)\rho. \tag{2.3.7}$$

The initial conditions, when $\xi = 0$, are

$$a(0, \eta, \theta) = 0, \tag{2.3.8}$$

$$t(0, \eta, \theta) = \eta, \tag{2.3.9}$$

$$x(0, \eta, \theta) = \theta, \tag{2.3.10}$$

$$\rho(0, \eta, \theta) = B(\eta, \theta), \tag{2.3.11}$$

When (2.3.5) is solved, then it can be seen that $a = \xi + f(\eta, \theta)$. Because of (2.3.8), it follows that $f(\eta, \theta) = 0$, so

$$a = \xi. \tag{2.3.12}$$

When (2.3.4) is solved, it can be seen that $t = \xi + g(\eta, \theta)$, and because of (2.3.9), it follows that $g(\eta, \theta) = \eta$, so

$$t = \xi + \eta, \tag{2.3.13}$$

and therefore

$$\eta = t - a. \tag{2.3.14}$$

From (2.3.6), and using what was just determined about t, it follows that

$$\frac{\partial x}{\partial \xi} = v(\xi + \eta), \tag{2.3.15}$$

so

$$x = \int_0^{\xi} v(\xi + \eta) d\xi \quad + h(\eta, \theta). \tag{2.3.16}$$

Now let $u = \xi + \eta$, and make the appropriate limit changes to yield

$$x = \int_{\eta}^{\xi+\eta} v(u) du + h(\eta, \theta) \tag{2.3.17}$$

$$= \int_{t-a}^{t} v(u) du + h(\eta, \theta). \tag{2.3.18}$$

When $a = 0$, it follows from (2.3.10) that $x = \theta$, so $h(\eta, \theta) = \theta$. Therefore,

$$x = \int_{t-a}^{t} v(u)du + \theta, \tag{2.3.19}$$

and so

$$\theta = x - \int_{t-a}^{t} v(u)du. \tag{2.3.20}$$

Beginning with (2.3.7), it yields

$$\frac{\partial \rho}{\partial \xi} = -\mu_s(\xi)\rho, \tag{2.3.21}$$

$$\frac{1}{\rho}d\rho = -\mu_s(\xi)d\xi, \tag{2.3.22}$$

$$\int_{B(\eta,\theta)}^{\rho(\xi,\eta,\theta)} \frac{1}{\rho}d\rho = -\int_0^{\xi} \mu_s(\xi)d\xi, \tag{2.3.23}$$

$$log\left(\rho(\xi,\eta,\theta)\right) - log\left(B(\eta,\theta)\right) = -\int_0^{\xi} \mu_s(\xi)d\xi, \tag{2.3.24}$$

$$\rho(\xi,\eta,\theta) = B(\eta,\theta)e^{-\int_0^{\xi}\mu_s(\xi)d\xi}. \tag{2.3.25}$$

Now transform back to the original variables using (2.3.12), (2.3.14), and (2.3.20), and insert a dummy variable in the integral to see that

$$\rho(a,t,x) = B\left(t-a, x - \int_{t-a}^{t} v(u)\,du\right) e^{-\int_0^a \mu_s(w)\,dw}. \tag{2.3.26}$$

The biological interpretation of this solution makes sense. If one wants to know the density of larvae of a specific age a, at a particular location x, at time t, one looks back in time to see how many were born at the time $t - a$ in the location that would force them to arrive at this location, x, at time t, and then finally one accounts for any that may have settled already.

Resource managers may not be interested in larval densities, but might be most concerned with how many green crabs settle at a particular location, over a specific time period, such as a season, a year, or several years. Call this accumulated abundance $\tau(x, t^\star)$, where

the beginning of the time period in question is set to $t = 0$. To determine $\tau(x, t^\star)$, integrate over the time period in question, 0 to $t^\star$, and all possible ages that may have settled, 0 to ∞. Since this is a continuous function over space as well, to obtain the number of larvae, also integrate over the spatial unit of interest, such as the width of the entrance to a bay, which is designated as the positive quantity $\triangle x$.

$$\tau(x, t^\star) = \int_x^{x+\triangle x} \int_0^{t^\star} \int_0^{\infty} \rho(a, t, x)\, \mu_s(a)\, da\, dt\, dx \tag{2.3.27}$$

$$= \int_x^{x+\triangle x} \int_0^{t^\star} \int_0^{\infty} \left[B\left(t - a, x - \int_{t-a}^{t} v(u)\, du \right) e^{-\int_0^a \mu_s(w)\, dw} \right] \mu_s(a)\, da\, dt\, dx. \tag{2.3.28}$$

2.4 Analysis of the Model

To fully understand this solution, functions must be defined for the current velocity and settlement, $v(t)$ and $\mu_s(a)$, as well as for birth of larvae, $B(t, x)$. This particular analysis, is more concerned with the effects of different velocity functions. Therefore it can be assumed that larvae are released at a constant rate and from a single source, San Francisco Bay. The coordinate system is defined such that $x = 0$ corresponds to San Francisco Bay, and positive values of x correspond to kilometers north of San Francisco. Hence, in this scenario, B is really a delta function,

$$B(t, x) = \delta(x)\,, \forall\, t. \tag{2.4.1}$$

μ_s can be thought of as a hazard function describing the odds of a particular larva settling out given that the larva has not settled out yet,

$$\mu_s = \frac{F'(a)}{1 - F(a)} \tag{2.4.2}$$

$$= \frac{f(a)}{1 - \int_0^a f(x)\, dx}\,, \tag{2.4.3}$$

where $f(a)$ is a probability density function describing the probability of a larva settling out at a particular age, a. Part of (2.3.28) can now be examined,

$$\mu_s(a)e^{-\int_0^a \mu_s(w)\,dw} = \frac{F'(a)}{1-F(a)}e^{-\int_0^a \frac{F'(w)}{1-F(w)}\,dw}. \tag{2.4.4}$$

Now let $u = 1 - F(w)$, so $du = -F'(w)$. Rewrite the integral as $\int \frac{du}{u}$, which can then be solved to show that

$$\begin{aligned}
\mu_s(a)e^{-\int_0^a \mu_s(w)\,dw} &= \frac{F'(a)}{1-F(a)}e^{ln\left(\frac{1-F(a)}{1-F(0)}\right)} && (2.4.5)\\
&= \frac{F'(a)}{1-F(a)}\frac{1-F(a)}{1-F(0)} && (2.4.6)\\
&= F'(a) && (2.4.7)\\
&= f(a). && (2.4.8)
\end{aligned}$$

In doing this, it is assumed that $F(0) = 0$. Since $F(0)$ is the cumulative number of larvae that have settled at time 0, this is entirely appropriate. The cumulative density function now looks like

$$\begin{aligned}
\tau(x,t^\star) &= \int_x^{x+\triangle x}\int_0^{t^\star}\int_0^{\infty} B\left(t-a, x-\int_{t-a}^{t} v(u)\,du\right) f(a)\,da\,dt\,dx && (2.4.9)\\
&= \int_x^{x+\triangle x}\int_0^{t^\star}\int_0^{\infty} \delta\left(x-\int_{t-a}^{t} v(u)\,du\right) f(a)\,da\,dt\,dx. && (2.4.10)
\end{aligned}$$

Now some velocity functions can be defined. First take the simplest case, when velocity is constant, so $v(t) = k$. To find τ, incorporate (2.4.1) into (2.4.9), and replace the velocity

function with a constant, k. As a result,

$$\tau(x,t^\star) = \int_x^{x+\triangle x}\int_0^{t^\star}\int_0^{\infty} \delta\left(x - \int_{t-a}^{t} v(u)\,du\right) f(a)\,da\,dt\,dx \tag{2.4.11}$$

$$= \int_x^{x+\triangle x}\int_0^{t^\star}\int_0^{\infty} \delta\left(x - \int_{t-a}^{t} k\,du\right) f(a)\,da\,dt\,dx \tag{2.4.12}$$

$$= \int_x^{x+\triangle x}\int_0^{t^\star}\int_0^{\infty} \delta\left(x - ka\right) f(a)\,da\,dt\,dx \tag{2.4.13}$$

$$= t^\star \int_x^{x+\triangle x}\int_0^{\infty} \delta\left(x - ka\right) f(a)\,da\,dx \tag{2.4.14}$$

$$= t^\star \int_0^{\infty} f(a) \int_x^{x+\triangle x} \delta\left(x - ka\right)\,dx\,da. \tag{2.4.15}$$

By the definition of a delta function,

$$\int_x^{x+\triangle x} \delta\left(x - ka\right)\,dx = \begin{cases} 1, \text{ if } \frac{x}{k} \le a \le \frac{x+\triangle x}{k} \text{ and } k > 0, \\ 1, \text{ if } \frac{x}{k} \ge a \ge \frac{x+\triangle x}{k} \text{ and } k < 0, \\ 0, \text{ otherwise.} \end{cases} \tag{2.4.16}$$

It will be assumed that $k > 0$, since the primary concern for this analysis is the northern transport of larvae. Therefore,

$$\tau(x,t^\star) = t^\star \int_{\frac{x}{k}}^{\frac{x+\triangle x}{k}} f(a)\,da. \tag{2.4.17}$$

Now a family of settling functions for $f(a)$ can be explored. One possibility is to assume that $f(a)$ comes from a family of gamma probability density functions, such that

$$f_n(a) = \frac{\alpha n\,(\alpha n a)^{n-1}}{(n-1)!} e^{-\alpha n a}. \tag{2.4.18}$$

This family of density functions was examined because by manipulating n, $f_n(a)$ can be shifted from an exponential to a delta function. (See Figure 2.2). When $n = 1$, then

$f_n(a) = \alpha e^{-\alpha a}$. Incorporating this into (2.4.17) yields

$$\tau(x, t^\star) = t^\star \int_{\frac{x}{k}}^{\frac{x+\triangle x}{k}} f(a)\, da \tag{2.4.19}$$

$$= t^\star \int_{\frac{x}{k}}^{\frac{x+\triangle x}{k}} \alpha e^{-\alpha a}\, da \tag{2.4.20}$$

$$= t^\star \left(e^{\frac{-\alpha x}{k}} - e^{\frac{-\alpha[x+\triangle x]}{k}} \right) \tag{2.4.21}$$

$$= t^\star \left[e^{\frac{-\alpha x}{k}} \left(1 - e^{\frac{-\alpha \triangle x}{k}} \right) \right]. \tag{2.4.22}$$

It is interesting to note that this particular case, when $n = 1$, leads to a constant settling rate. This result can be seen by looking back at (2.4.3).

$$\mu_s(a) = \frac{f_1(a)}{1 - \int_0^a f_1(x)\, dx} \tag{2.4.23}$$

$$= \frac{\alpha e^{-\alpha a}}{1 - \int_0^a \alpha e^{-\alpha x}\, dx} \tag{2.4.24}$$

$$= \frac{\alpha e^{-\alpha a}}{1 - (-e^{-\alpha a} + 1)} \tag{2.4.25}$$

$$= \alpha. \tag{2.4.26}$$

However, *C. maenas* larvae probably do not settle at a constant rate, since they must develop through four zoeal stages and one megalopae stage before being competent to settle. The rate at which they develop is determined by temperature (Dawirs 1985, deRivera et al. 2007). To simplify this problem, assume a constant temperature, so that the larvae will all develop at the same rate, and therefore they will be competent to settle at a specific age, a_0. If it is assumed that the larvae settle as soon as they are competent, then this assumption could be modeled by allowing $n = \infty$, which transforms $f_n(a)$ into a delta function, $f_n(a) = \delta(a - a_0)$. This is equivalent to setting $a_0 = \frac{1}{\alpha}$, to relate back to (2.4.18).

Turning back to (2.4.17), it can be seen that

$$\tau(x,t^\star) = t^\star \int_{\frac{x}{k}}^{\frac{x+\triangle x}{k}} f_n(a)\,da \tag{2.4.27}$$

$$= t^\star \int_{\frac{x}{k}}^{\frac{x+\triangle x}{k}} \delta(a-a_0)\,da \tag{2.4.28}$$

$$= \begin{cases} t^\star, \text{ if } \frac{x}{k} - a_0 \leq 0 \leq \frac{x+\triangle x}{k} - a_0, \\ 0, \text{ otherwise.} \end{cases} \tag{2.4.29}$$

$$\equiv \begin{cases} t^\star, \text{ if } ka_0 - \triangle x \leq x \leq ka_0, \\ 0, \text{ otherwise.} \end{cases} \tag{2.4.30}$$

So, if velocity is a constant, then all the larvae settle at the same location, no matter when they are released. That location is determined by the velocity, k, and the time it takes the larvae to develop, a_0, such that all the larvae settle at $x = ka_0$. However, when confronted with realistic oceanographic conditions, the assumption of constant velocity is not appropriate. ROMS is the Regional Ocean Model System used by many in the scientific community to approximate the movement, temperature, salinity, mixing and other characteristics of large oceans (Hermann and Musgrave 2006). Based on the ROMS output, the velocity is clearly not constant over time (see Figure 2.3). Therefore, it seems appropriate to investigate other possible velocity functions.

Going back to the birth function, it can be expressed as a uniform function around a small area near San Francisco,

$$B\left(x - g(t,a_0)\right) = \begin{cases} \frac{1}{\epsilon}(b), \text{ if } |x - g(t,a_0)| \leq \frac{\epsilon}{2}, \\ 0, \text{ otherwise,} \end{cases} \tag{2.4.31}$$

where b is the number of larvae released from San Francisco Bay each day. As $\epsilon \to 0$, this birth function approaches a δ-function, so it is similar to the former assumption that all larvae were released from a single point in space, (2.4.1). Now assume that the velocity

function, $v(t)$ is periodic with a period of d days. This function could be expressed as

$$v(t) = \beta_0 + \beta_1 \cos(\lambda t) + \beta_2 \sin(\lambda t), \tag{2.4.32}$$

where $\lambda = \frac{2\pi}{d}$. Integrating from $t - a$ to t yields

$$\begin{aligned}
\int_{t-a}^{t} v(u)\, du &= \int_{t-a}^{t} \beta_0 + \beta_1 \cos(\lambda u) + \beta_2 \sin(\lambda u)\, du && (2.4.33)\\
&= \beta_0 a + \beta_1 \int_{t-a}^{t} \cos(\lambda u)\, du + \beta_2 \int_{t-a}^{t} \sin(\lambda u)\, du && (2.4.34)\\
&= \beta_0 a + \frac{\beta_1}{\lambda} \left[\sin(\lambda t) - \sin(\lambda t - \lambda a)\right] - \frac{\beta_2}{\lambda} \left[\cos(\lambda t) - \cos(\lambda t - \lambda a)\right] && (2.4.35)\\
&= g(t, a). && (2.4.36)
\end{aligned}$$

Values for $\vec{\beta}$ can be estimated by fitting (2.4.32) to ROMS output (see Figure 2.3). The density of settling crabs at a particular location can now be examined by looking back to (2.4.9),

$$\begin{aligned}
\tau(x, t^\star) &= \int_{x}^{x+\triangle x} \int_{0}^{t^\star} \int_{0}^{\infty} B\left(x - \int_{t-a}^{t} v(u)\, du\right) f(a)\, da\, dt\, dx && (2.4.37)\\
&= \int_{x}^{x+\triangle x} \int_{0}^{t^\star} \int_{0}^{\infty} B\left(x - g(t, a)\right) f(a)\, da\, dt\, dx. && (2.4.38)
\end{aligned}$$

If it is again assumed that $f(a) = \delta(a - a_0)$, then by using the sifting property of the δ-function, the first inside integral can be solved to give

$$\begin{aligned}
\tau(x, t^\star) &= \int_{x}^{x+\triangle x} \int_{0}^{t^\star} \int_{0}^{\infty} B\left(x - g(t, a)\right) \delta(a - a_0)\, da\, dt\, dx && (2.4.39)\\
&= \int_{x}^{x+\triangle x} \int_{0}^{t^\star} B\left(x - g(t, a_0)\right)\, dt\, dx. && (2.4.40)
\end{aligned}$$

The primary concern is the number of larvae settling at a particular location, x, so x can be treated as fixed for the inside integral. Thus, the birth function now has only one variable, t. If the velocity function is such that larvae never reach the location x, then $\tau(x, t^\star) = 0$

for all values of $t^\star$. If larvae can reach x, and yet $B(x - g(t^\star, a_0)) = 0$, then

$$\int_0^{t^\star} B\left(x - g(t, a_0)\right)\, dt = c\,(b), \tag{2.4.41}$$

where $c \in \mathbb{Z}$. Moving on to the next integral, it can be seen that

$$\tau(x, t^\star) = \int_x^{x+\triangle x} c(b)\; dx \tag{2.4.42}$$

$$= (c \times b)(\triangle x). \tag{2.4.43}$$

If $B(x - g(t^\star, a_0)) \neq 0$, then the solution will have some fraction added to c; $(c+\varepsilon)(b)(\triangle x)$.

2.5 Discussion

Resource managers, as well as mariculturists and fishermen, are interested in knowing what sort of ocean conditions may transport *C. maenas* larvae to various estuaries on the west coast in a given year. This advection and age-structured model can be used to determine what ocean conditions are required in order to advect larvae from a known source location, such as San Francisco Bay, to a given location.

Willapa Bay is approximately 990 km north of San Francisco Bay. Located in southwestern Washington, Willapa Bay is the center of Washington State's farmed oyster industry. A first-year class of European green crab arrived in Willapa Bay during the El-Niño event of 1997–98.

Assuming a constant velocity, $v(t) = k$, and a constant larval duration, $a_0 = 65$ days, results in the conclusion that the larvae hatched in San Francisco Bay would need to travel at an average speed of 15 km/day, or 0.17 m/sec, to reach Willapa Bay and settle there. If the larval duration is 75 days, then the average northern velocity needed to reach Willapa Bay is only 13 km/day, or 0.15 m/sec.

As the parameters of the settling pdf, $f_n(a)$, shift, the range of larval durations increases from one age to a range of ages. Therefore, although the mean larval duration may still be a_0, there is an increasing chance that some larvae will remain in the ocean for longer than a_0, potentially allowing them to be advected further north. Based on a recent analysis of an

individual-based model (IBM), a potential settling function can be fit to the model results (Figure 2.4). The larval durations range from 45 to 75 days. The parameters used to fit the model results are $n = 50$ and $\alpha = 0.02$.

The oceanographic currents from the same IBM can be used to fit a simple harmonic velocity function as described earlier (2.4.32) (see Figure 2.3). Green crab larvae are usually found in the water year-round in their southern range of eastern North America and Europe, so the specific days larvae would need to be released to settle a certain distance away from San Francisco can be examined. Take a simple case when $a_0 = 65$, $\epsilon = .5$, and assume one is interested in the number of larvae that settle at a point 290 km north of San Francisco ($x = 290$), between January 1, 1997 and July 1, 1999 ($t^\star = 911$, since $t = 0$ corresponds to January 1, 1997). (2.4.41) can then be solved to give $c = 3$ (see Figure 2.5). Only larvae released during three distinct days in that two-and-a-half-year time span will settle at the location of interest, x. Those days are December 4, 1997; December 4, 1998; and December 30, 1998. Managers responsible for estuaries located close to 290 km north of San Francisco should therefore be concerned with larvae that are released in December.

Humboldt Bay is approximately 330 km north of San Francisco, and was invaded by green crabs in 1994. However, according to this model, fitted to the ROMS data from 1997–2003, *C. maenas* larvae would never reach that far north from San Francisco. On the other hand, the velocity function that was used is somewhat simplistic and does not account for interannual variation of ocean conditions such as El Niño events. (Note the failure of the fitted function to account for the peak velocity in 1997–98 in Figure 2.3). This kind of oceanographic variation could supply larvae to Humboldt Bay from San Francisco during certain years.

The model could be extended in several different ways. Certainly more work could be done with the velocity function. The harmonic model discussed above could be expanded to include the sums of several sines and cosines, making it more complicated, but potentially more realistic by trying to capture that interannual variation. The velocity could also be modeled as an autocorrelation function, which could result in similar or vastly different results. The accuracy of any velocity model will depend on the quality and quantity of oceanographic data that can be used to parameterize an appropriate velocity function. In

addition, the velocity function could be expanded to two dimensions, $v(x,t)$, to capture spatial and temporal variability in ocean currents. This function might make the model analytically intractable, depending on how that velocity function is defined, but a numerical analysis might still be possible.

This model could also be rewritten to include diffusion. The diffusion term could be interpreted in several ways. Throughout the model analysis so far, all larvae that are released at a particular moment in time are assumed to travel together. Diffusion could represent a spreading out of that larval cohort in space, based on the larvae swimming horizontally. Alternatively, the diffusion constant could capture some of the variability of the ocean current. Green crab larvae generally travel in the top 30 meters of the water column, and the velocity is not uniform throughout that column. Diffusion could therefore capture the variability of ocean conditions that larvae experience as they migrate vertically in the water column. Incorporating diffusion adds another large layer of complexity to the model, but it could help capture more of the biologic reality, and the results might be quite different. Parameterizing the diffusion coefficient could be difficult, as seen in the model employed by Polovina et al. (1999), but drifter data may help.

2.6 Conclusion

An advection and age-structured model aimed at modeling larval dispersal and settling was proposed and successfully solved. This model accounts for the advection due to ocean currents, including potential variation in those currents. It also accounts for larval development, by determining when larvae are competent to settle based on their age. The variation in larval development can be captured by thinking of $\mu_s(a)$ as a hazard function, and using a settlement pdf, $f(a)$, from the gamma family. The variability of the ocean currents can be partially captured by employing harmonic functions with various degrees of complexity.

2.7 Figures

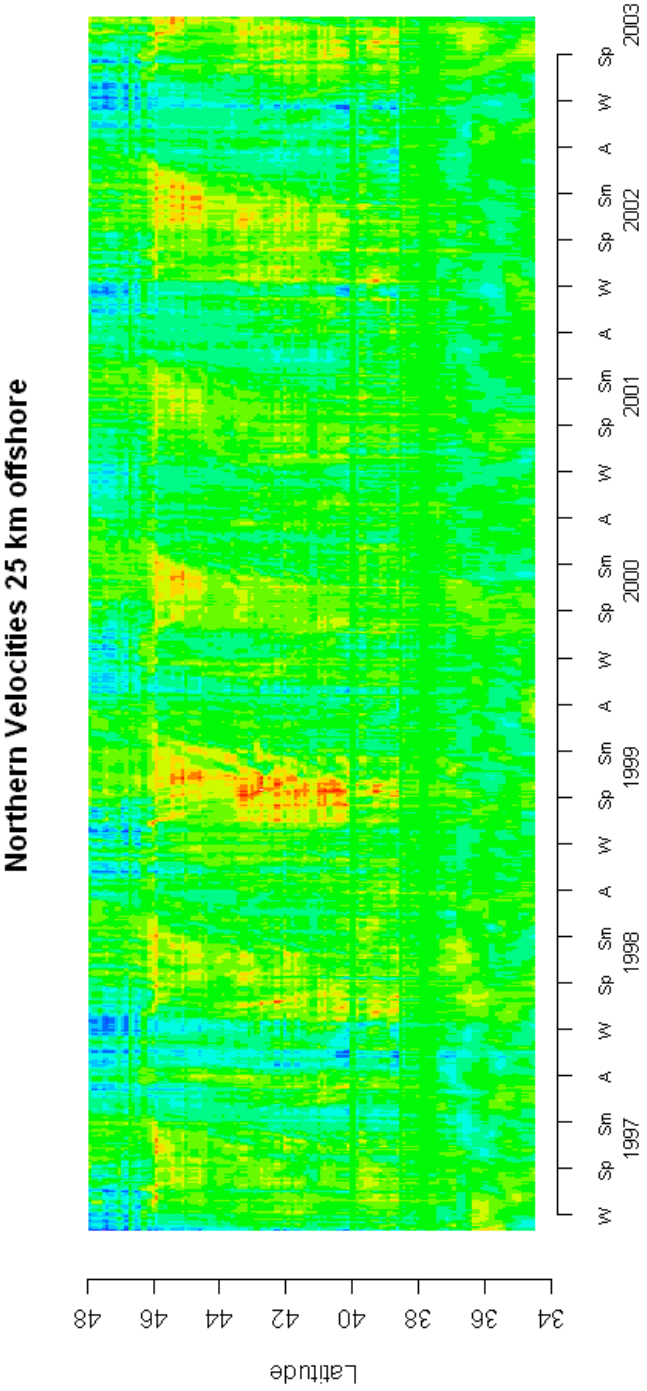

Figure 2.1: Ocean velocities over space and time, based on ROMS output from 25 km offshore. Blues depict northern currents; reds depict southern currents. Greens are very low velocity currents.

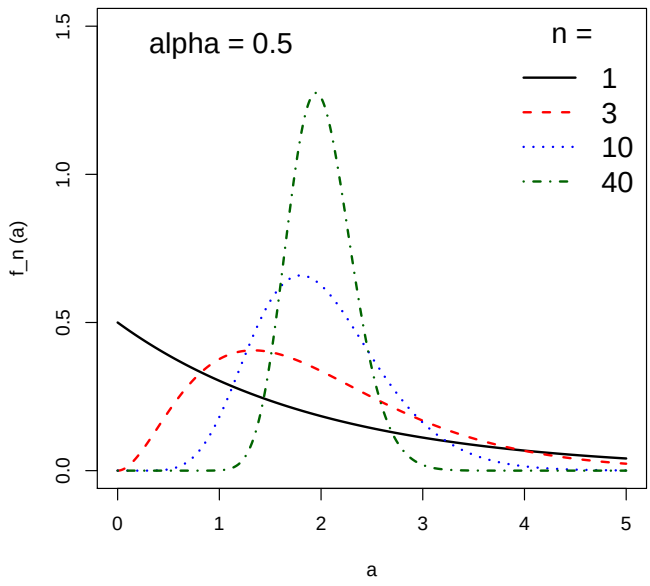

Figure 2.2: This shows how as n increases, $f_n(a)$ moves from an exponential function to a delta function.

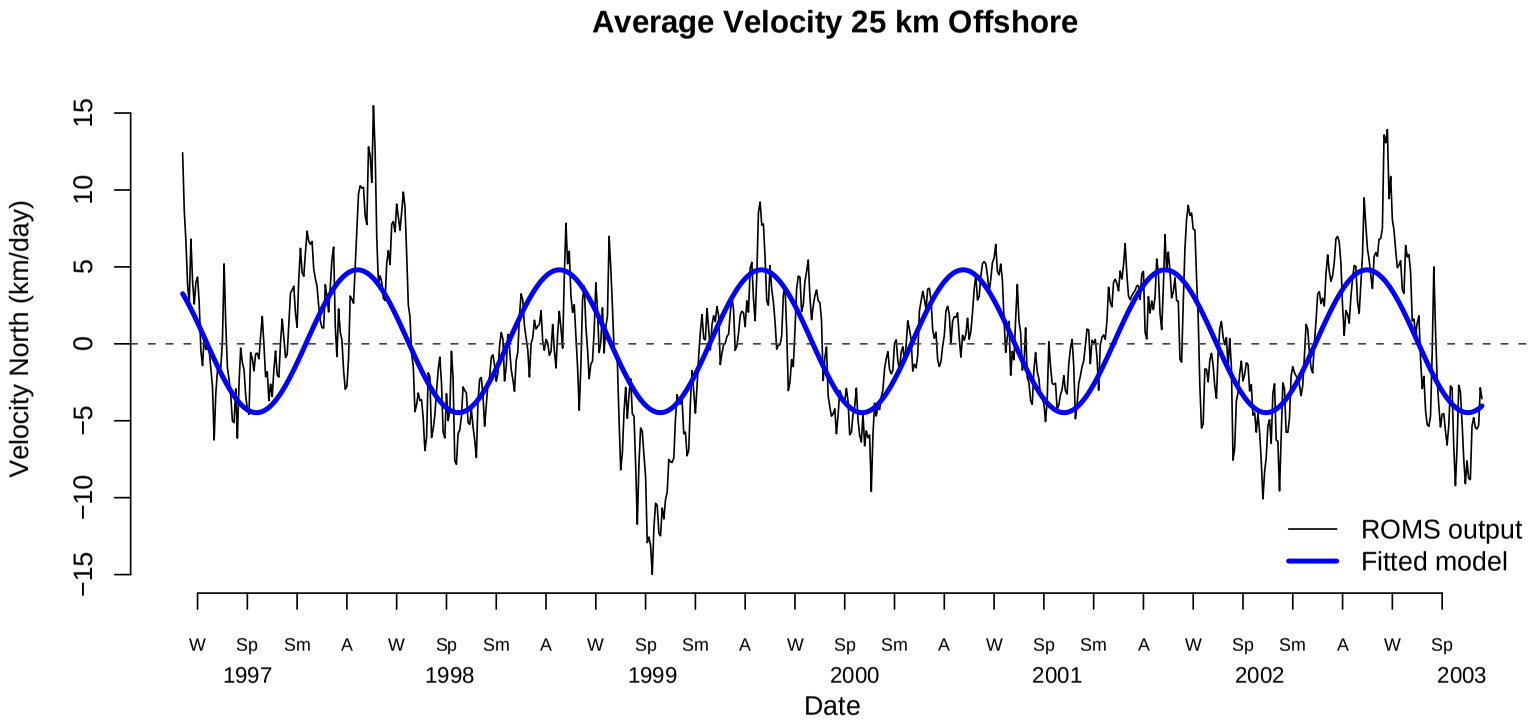

Figure 2.3: This is the average velocity 25 km off the west coast, as provided by ROMS, and a fitted model, $v(t)$, to that output.

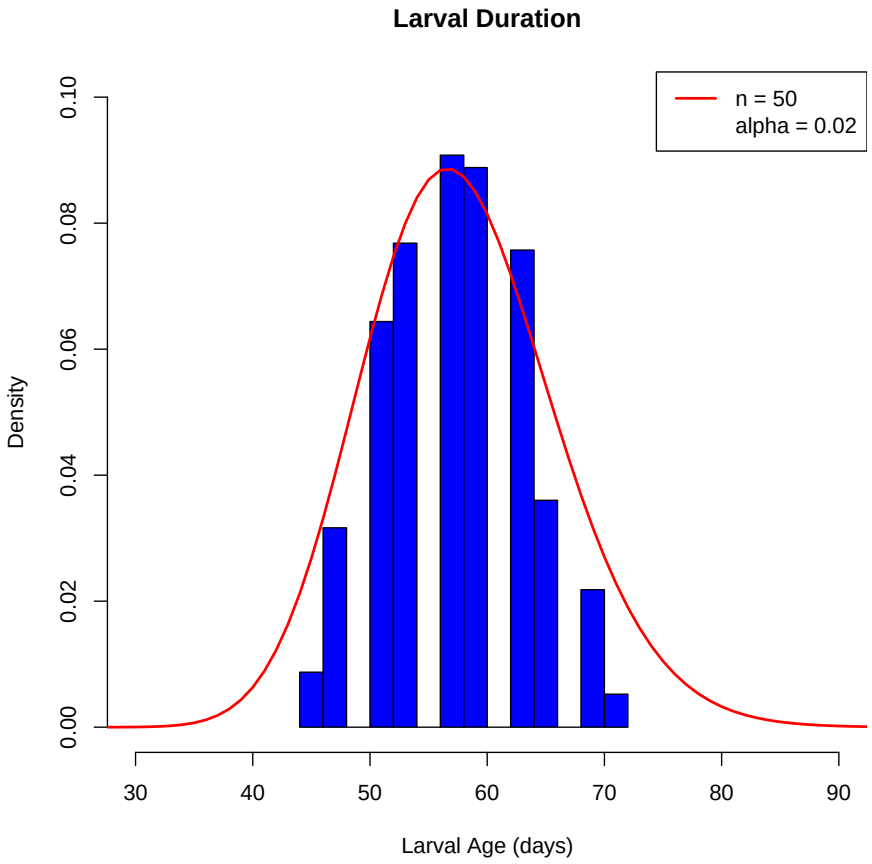

Figure 2.4: Results of an individual-based model that simulated larval advection and development based on ocean currents and temperatures 25 km offshore, and a fitted settling pdf, $f_n(a)$ (red line).

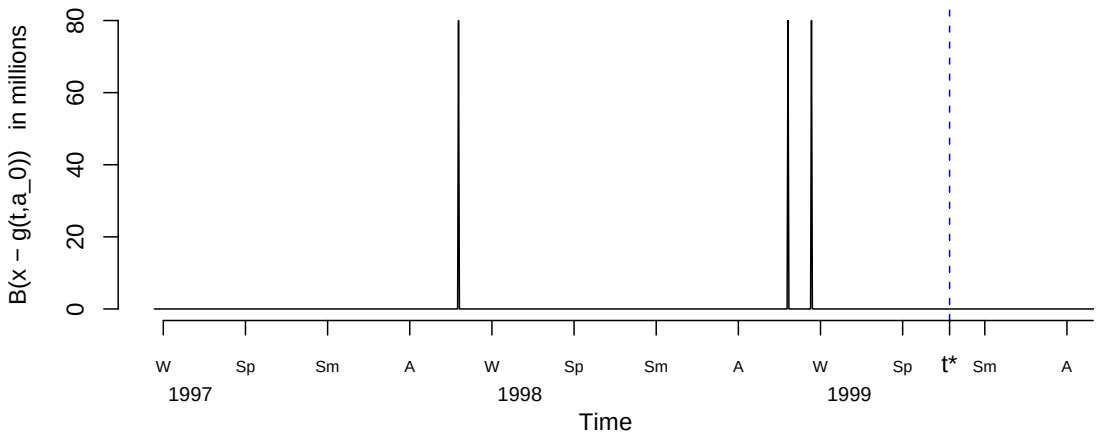

Figure 2.5: Using the fitted velocity function, $B(x - g(t, a_0))$ is plotted over time. Given $t^\star = 881$, it can be seen that $c = 3$, corresponding to the three peaks in the plot. Integrating over each peak yields b.

BIBLIOGRAPHY

Berrill, M. (1982). The life cycle of the green crab *Carcinus maenas* at the northern end of its range. *Journal of Crustacean Biology*, 2(1):31–39.

Carlton, J. T. and Cohen, A. N. (2003). Episodic global dispersal in shallow water marine organisms: the case history of the European shore crabs *Carcinus maenas* and *C. aestuarii*. *Journal Of Biogeography*, 30(12):1809–1820.

Cohen, A. N., Carlton, J. T., and Fountain, M. C. (1995). Introduction, dispersal and potential impacts of the green crab *Carcinus maenas* in San Francisco Bay, California. *Marine Biology*, 122(2):225–237.

Cunningham, P. N. and Hughes, R. N. (1984). Learning of predatory skills by shorecrabs *Carcinus maenas* feeding on mussels and dogwhelks. *Marine Ecology-Progress Series*, 16(1-2):21–26.

Dawirs, R. R. (1985). Temperature and larval development of *Carcinus-maenas* (decapoda) in the laboratory - predictions of larval dynamics in the sea. *Marine Ecology-Progress Series*, 24(3):297–302.

deRivera, C. E., Hitchcock, N. G., Teck, S. J., Steves, B. P., Hines, A. H., and Ruiz, G. M. (2007). Larval development rate predicts range expansion of an introduced crab. *Marine Biology*, 150(6):1275–1288.

Elner, R. W. (1978). Mechanics of predation by shore crab, *Carcinus maenas* (L), on edible mussel, *Mytilus edulis* (L). *Oecologia*, 36(3):333–344.

Glude, J. B. (1955). The effects of temperature and predators on the abundance of the soft-shell clam, *Mya arenaria*, in New England. *Transactions of the American Fisheries Society*, 84(1):13–26.

Grimm, V. and Railsback, S. F. (2005). *Individual-based Modeling and Ecology*. Princeton University Press, Princeton.

Grosholz, E. D. (1996). Contrasting rates of spread for introduced species in terrestrial and marine systems. *Ecology*, 77(6):1680–1686.

Grosholz, E. D. and Ruiz, G. M. (1995). Spread and potential impact of the recently introduced European green crab, *Carcinus maenas*, in central California. *Marine Biology*, 122(2):239–247.

Grosholz, E. D. and Ruiz, G. M. (1996). Predicting the impact of introduced marine species: Lessons from the multiple invasions of the European green crab *Carcinus maenas*. *Biological Conservation*, 78(1-2):59–66.

Grosholz, E. D. and Ruiz, G. M. (2002). Management plan for the European green crab. Technical report, Aquatic Nuisance Species Task Force.

Grosholz, E. D., Ruiz, G. M., Dean, C. A., Shirley, K. A., Maron, J. L., and Connors, P. G. (2000). The impacts of a nonindigenous marine predator in a California bay. *Ecology*, 81(5):1206–1224.

Hermann, A. J. and Musgrave, D. L. (2006). Evaluation of ocean circulation models for the Bering Sea and Aleutian Islands region. Technical report, NPRB. North Pacific Research Board Final Report 402, 51 pp.

Hickey, B. M. and Banas, N. S. (2003). Oceanography of the US Pacific Northwest Coastal Ocean and estuaries with application to coastal ecology. *Estuaries*, 26(4B):1010–1031.

Jamieson, G., Foreman, M., Cherniawsky, J., and Levings, C. (2002). *Crabs in cold water regions : biology, management, and economics*, chapter European Green Crab (*Carcinus maenas*) Dispersal: The Pacific Experience, pages 561–576. University of Alaska Sea Grant, Fairbanks, Alaska.

Jamieson, G. S., Grosholz, E. D., Armstrong, D. A., and Elner, R. W. (1998). Potential ecological implications from the introduction of the European green crab, *Carcinus maenas* (linneaus), to British Columbia, Canada, and Washington, USA. *Journal of Natural History*, 32(10-11):1587–1598.

Kobayashi, D. R. (2006). Colonization of the Hawaiian Archipelago via Johnston Atoll: a characterization of oceanographic transport corridors for pelagic larvae using computer simulation. *Coral Reefs*, 25(3):407–417. Kobayashi, Donald R. 37.

Kobayashi, D. R. and Polovina, J. J. (2006). *Northwestern Hawaiian Islands Third Scientific Symposium: November 2-4, 2004*, chapter Simulated seasonal and interannual variability in larval transport and oceanography in the Northwestern Hawaiian Islands using satellite remotely sensed data and computer modeling, pages 365–390. Number 543. National Museum of Natural History.

Lafferty, K. D. and Kuris, A. M. (1996). Biological control of marine pests. *Ecology*, 77(7):1989–2000.

Lowe, S., Browne, M., Boudjelas, S., and De Poorter, M. (2000). 100 of the worlds worst invasive alien species a selection from the global invasive species database. The Invasive Species Specialist Group.

McDonald, P. S., Jensen, G. C., and Armstrong, D. A. (2001). The competitive and predatory impacts of the nonindigenous crab *Carcinus maenas* (L.) on early benthic phase Dungeness crab *Cancer magister* Dana. *Journal of Experimental Marine Biology and Ecology*, 258(1):39–54.

Miller, T. W. (1996). First record of the green crab, *Carcinus maenas*, in Humboldt Bay, California. *California Fish and Game*, 82(2):93–96.

Miron, G., Audet, D., Landry, T., and Moriyasu, M. (2005). Predation potential of the invasive green crab (*Carcinus maenas*) and other common predators on commercial bivalve species found on Prince Edward Island. *Journal of Shellfish Research*, 24(2):579–586.

Mohamedeen, H. and Hartnoll, R. G. (1989). Larval and postlarval growth of individually reared specimens of the common shore crab *Carcinus maenas* (L). *Journal Of Experimental Marine Biology And Ecology*, 134(1):1–24.

Nagaraj, M. (1993). Combined effects of temperature and salinity on the zoeal development of the green crab, *Carcinus maenas* (Linnaeus, 1758) (Decapoda: Portunidae). *Scientia Marina*, 57(1):1–8.

NOAA (2006). *North-East Pacific physical model output - subgrid C*. [Data file] Retrieved on October 20, 2006 from http://ferret.pmel.noaa.gov/FOCI/servlets/dataset.

Palacios, K. C. and Ferraro, S. P. (2003). Green crab (*Carcinus maenas* linnaeus) consumption rates on and prey preferences among four bivalve prey species. *Journal of Shellfish Research*, 22(3):865–871.

Polovina, J. J., Kleiber, P., and Kobayashi, D. R. (1999). Application of TOPEX-POSEIDON satellite altimetry to simulate transport dynamics of larvae of spiny lobster, *Panulirus marginatus* in the Northwestern Hawaiian Islands, 1993-1996. *Fishery Bulletin*, 97(1):132–143.

Queiroga, H. (1996). Distribution and drift of the crab *Carcinus maenas* (L) (Decapoda, Portunidae) larvae over the continental shelf off northern Portugal in April 1991. *Journal Of Plankton Research*, 18(11):1981–2000.

Queiroga, H. (1998). Vertical migration and selective tidal stream transport in the megalopa of the crab *Carcinus maenas*. *Hydrobiologia*, 376:137–149.

Queiroga, H., Almeida, M. J., Alpuim, T., Flores, A. A. V., Francisco, S., Gonzalez-Gordillo, I., Miranda, A. I., Silva, I., and Paula, J. (2006). Tide and wind control of megalopal supply to estuarine crab populations on the Portuguese west coast. *Marine Ecology-Progress Series*, 307:21–36.

Queiroga, H., Moksnes, P. O., and Meireles, S. (2002). Vertical migration behaviour in the larvae of the shore crab *Carcinus maenas* from a microtidal system (Gullmarsfjord, Sweden). *Marine Ecology-Progress Series*, 237:195–207.

Rooper, C. N., Gunderson, D. R., and Hickey, B. M. (2006). An examination of the feasibility of passive transport from coastal spawning grounds to estuarine nursery areas for English sole. *Estuarine Coastal and Shelf Science*, 68(3-4):609–618.

Strub, P. T., Allen, J. S., Huyer, A., and Smith, R. L. (1987a). Large-scale structure of the spring transition in the coastal ocean off western North America. *Journal of Geophysical Research-Oceans*, 92(C2):1527–1544.

Strub, P. T., Allen, J. S., Huyer, A., Smith, R. L., and Beardsley, R. C. (1987b). Seasonal cycles of currents, temperatures, winds, and sea-level over the northeast Pacific continental shelf - 35 degrees N to 48 degrees N. *Journal of Geophysical Research-Oceans*, 92(C2):1507–1526.

Wonham, M. J. and Carlton, J. T. (2005). Trends in marine biological invasions at local and regional scales: the northeast Pacific Ocean as a model system. *Biological Invasions*, 7(3):369–392.

Yamada, S. B., Dumbauld, B. R., Kalin, A., Hunt, C. E., Figlar-Barnes, R., and Randall, A. (2005). Growth and persistence of a recent invader *Carcinus maenas* in estuaries of the northeastern Pacific. *Biological Invasions*, 7(2):309–321.

Yamada, S. B., Hunt, C., and Richmond, N. (1999). The arrival of the European green crab, *Carcinus maenas*, in Oregon estuaries. In Pederson, J., editor, *Marine Bioinvasions: Proceedings for the First National Conference January 24-27, 1999*, pages 94–99. Massachusetts Institute of Technology Sea Grant College Program.

APPENDIX: R CODE FOR IBM

Accessing and Creating ROMS output

```
# get velocity and temperature data for a given longitude
readData <- function(long) {
        all.data <- as.data.frame(read.csv(paste('//Users//
kevinsee//Documents//UW_documents//Green Crab//
Data//ROMS data//LASoutput_', long, '.csv', sep=''),
header = T, col.names=c('date', paste('N',seq(30, 48, .1),
 sep=''))))
        all.data
}
# get coordinates of entire coastline
library(maps)
library(mapdata)
world.coords <- map('worldHires', xlim = c(-129, -119),
 ylim = c(29, 55), fill=T, col='gray', plot=F)

# pull out coordinates of west coast
west.coast <- data.frame(x=world.coords$x[
 world.coords$x > -129 &  world.coords$x < -119 &
 world.coords$y > 29 & world.coords$y < 55],
 y=world.coords$y[world.coords$x > -129 &
 world.coords$x < -119 &  world.coords$y > 29 &
 world.coords$y < 55])
 coast <- data.frame(long = west.coast$x[west.coast$y<47
 | ( west.coast$y>47 & west.coast$x<(-123.15) ) &
 west.coast$y<49], lat = west.coast$y[west.coast$y<47 |
  ( west.coast$y>47 & west.coast$x<(-123.15) )  & west.coast$y<49])
coast <- na.omit(coast)

# this function gets the coastal longitude for a specific latitude
getCoastLong <- function(latitude)
{
        low.lat <- max(coast$lat[coast$lat<latitude])
        low.long <- min(coast$long[coast$lat == low.lat])
        high.lat <- min(coast$lat[coast$lat>latitude])
        high.long <- min(coast$long[coast$lat == high.lat])
        y <- c(low.long, high.long)
        x <- c(low.lat, high.lat)
        coeff <- coef(lm(y~x))
        coast.long <- coeff[1] + coeff[2]*latitude
        coast.long
}
```

```
# this will build a list of coastal longitudes that match up with the
  latitudes we have model output for

getCoastCoords <- function()
{
# southern limit of usa latitudes is 34.46, so we won't go below that
        lats <- seq(34.5, 48, .1)
        longs <- NULL
        for (i in 1:length(lats)) {
                longs[i] <- getCoastLong(lats[i])
        }

        # now get rid of two bizarre points, one in San Fran, one in
  Columbia River
        SF.long <- longs[lats==38.1]
        CR.long <- longs[lats==46.2]

        # this function returns new longtitude by examining .1 deg of
  latitude above and below set latitude
        NewLong <- function(lat)
        {
                x <- c(lat-.1, lat+.1)
                y <- c(longs[lats==x[1]], longs[lats==x[2]])
                new.fit <- coef(lm(y~x))
                new.long <- new.fit[1] + new.fit[2] * lat
                new.long
        }

        SF.long.new <- NewLong(38.1)

        # for some reason this wasn't working for Columbia River, so
  I forced it
        NewLong2 <- function(lat)
        {
                x <- c(lat-.1, lat+.1)
                y <- c(longs[lats==x[1]], longs[lats==46.3])
                new.fit <- coef(lm(y~x))
                new.long <- new.fit[1] + new.fit[2] * lat
                new.long
        }

        CR.long.new <- NewLong2(46.2)

        longs[lats==38.1] <- SF.long.new
        longs[lats==46.2] <- CR.long.new

        data.frame(lat = lats, long = longs)
}
coastCoords <- getCoastCoords()
```

```
# this function determines how many deg of longitude a set
  distance (dist) in km is at a given latitude (lat)
getLongDeg <- function(dist, lat) {
        # radius of earth in km
        rad.Earth <- 6378.135
        diffOneDegLong <- (pi/180) * rad.Earth * cos(lat/(180/pi))
        DegDist <- dist / diffOneDegLong
        DegDist
}

# this function creates a list of coordinates a set distance (in km)
  off shore
createCoords <- function(dist) {
        lat <- coastCoords$lat
        long <- coastCoords$long
        for(i in 1:length(long)) {
                new.long <- long[i] - getLongDeg(dist, lat[i])
                long[i] <- new.long
        }
        coords <- data.frame(lat = lat, long = long)
        coords
}

# this function constructs a data table, based on distance
  offshore (in km), for
    all years that data is available
constructData <- function(dist)
{
        coords <- createCoords(dist)
        longs <- -ceiling(coords$long * 10) / 10
        # sets lower limit on longitudinal transects
        longs[longs < 122.4] <- 122.4
        x <- seq(30.0 - .1*(2), 48, .1)
        y <- seq(2, length(x)+1, 1)
        b.vel <- coef(lm(y~x))
        all.data <- data.frame(JulianDay = rep(c(seq(2,365,3),
    seq(3, 363, 3), seq(1, 364, 3), seq(2, 365, 3),
    seq(2, 365, 3), seq(3, 363, 3), seq(1, 160, 3)), 2),
    year=rep(c(rep(1997, 122), rep(1998, 121),
    rep(1999, 122), rep(2000, 122), rep(2001, 122),
    rep(2002, 121), rep(2003, 54)),2))
        for(i in 1:(length(longs)-1)) {
                data <- readData(longs[i])
                data.vector <- data[ , b.vel[1] + b.vel[2] *
    coords$lat[i]]
                # this line returns which i value is causing error
                if(length(data.vector) != length(all.data[,1])) print(i)
                all.data <- data.frame(all.data, data.vector)
        }
        colnames(all.data) <- c('JulianDay', 'year',
```

```
    paste('N',seq(34.5, 47.9, .1), sep=''))
        all.data
}
```

Model Functions

```
# The following functions help determine the larvae's movement
# to set the number of column based on latitude
# change the product of .1 and the number of columns before
the data start
x <- seq(34.5 - .1*(2), 47.9, .1)
y <- seq(2, length(x)+1, 1)
coeff <- coef(lm(y~x))

# this function returns the data (velocity or temperature) for a
particular latitude (lat) on a particular day (day) using a
dataframe (dataFile)
getDataPoint <- function(lat, day, dataFile) {
        dataPoint <- dataFile[dataFile$Day == day, coeff[1]-1 +
        coeff[2] * lat]
        dataPoint
}

## this function returns a weighted average of two velocities
or temperatures, at day = day, depending on actual latitude (x),
 and two readings around that (a and b) using a data frame (dataFile)
wtavg <- function(lat, day, dataFile){
        low.lat <- floor(lat*10)/10
        low.lat.reading <- getDataPoint(low.lat, day, dataFile)
        if (low.lat < 47.8) high.lat.reading <-
        getDataPoint(low.lat + .1, day, dataFile)
        else high.lat.reading <-getDataPoint(47.9, day, dataFile)
        # weight the distance x is from the ref latitude
        p <- (lat - low.lat)/ 0.1
        newDataPoint <- ( ( (1-p) * low.lat.reading) +
        (p * high.lat.reading) )
        newDataPoint
}

# this function computes the distance traveled from latitude = lat
starting at Julian day = day for 3 days and returns the change in
latitude in degrees using a velocity data frame (vel.data)
dist.traveled <- function(lat, day, vel.data){
        v <- wtavg(lat,day, vel.data)
#         calculates distance traveled for 3 days in kilometers
        dist.km <- v * (60 * 60 * 24 * 3) / 1000
#         converts to nautical miles
        dist.nm <- dist.km /  1.852
#         converts to latitude degrees
```

```
        dist.deg <- dist.nm / 60
        dist.deg
}


# The following function help determine the larvae's development
# calculates the percentage of development a larvae accomplishes in
each stage during one time step from data frame of temperatures (Temp)
based on deRivera (2006)
deRiveraDevelop <- function(lat, day, stage, Temp) {
        temp <- wtavg(lat, day, Temp)
        if(stage == 1) {
                a <- 122.96
                b <- -34.7
        }
        if(stage == 2) {
                a <- 77.76
                b <- -21.72
        }
        tot.develop.day <- a + (b * log(temp))
        # change numerator to whatever the timestep is in days
        timestep.percent <- 3 / tot.develop.day
        result <- timestep.percent
        result
}



# This function actually runs the model
# each time step, move each cohort of larvae, and calculate development
run.model <- function(velData, tempData, nstep, start.lat)
{
        output <- data.frame(dayReleased=NA, latitude=NA, stage=NA,
        devPercent=NA, totDevelopTime=NA)
        days <- seq(1,3*nstep,3)
        output[1,] <- c(velData[1,1],start.lat,1,0,0)
        for(i in 2:length(days))
        {
                for(j in 1:(i-1))
                {
                        if (output$devPercent[j] < 1 &&
                        output$stage[j] < 3)
                        {
        # larvae moves appropriate distance
                                distance <- dist.traveled(
                                output$latitude[j], days[i], velData)
                                new.lat <- output$latitude[j] + distance
                                # prevent larvae from difting
                                south of avail. data
                                if (new.lat < 34.5) new.lat <- 34.5
```

```
                                # prevent larvae from drifting
                                north of avail.data
                                if (new.lat > 47.9) new.lat <- 47.9
                                output$latitude[j] <- new.lat
        # larvae develops appropriate percentage
                                devPer <- deRiveraDevelop
                                (output$latitude[j], days[i],
                                output$stage[j], tempData)
                                output$devPercent[j] <-
                                output$devPercent[j] + devPer
        # larvae develops into megalopea if necessary
                                if(output$stage[j] == 1 &&
                                output$devPercent[j] >= 1)
                                {
                                        output$stage[j] <- 2
                                        output$devPercent[j] <-
                                        output$devPercent[j] - 1
                                }
        # larvae become fully developed and ready to settle
                                if(output$stage[j] == 2 &&
                                output$devPercent[j] >= 1)
                                {
                                        output$stage[j] <- 3
                                        output$devPercent[j] <- 1
                                        output$totDevelopTime[j] <-
                                        days[i] - output$dayReleased[j]
                                }
                        }
                }
                output <- as.data.frame(rbind(output,c(days[i],
                start.lat,1,0,0)))
        }
        output
}

# this function coverts distance in km into dec degrees latitude
convertKm2Deg <- function(dist.km)
{
        deg <- dist.km / (60 * 1.852)
        deg
}

# this function coverts dec degrees latitude into distance (km)
convertDeg2Km <- function(degrees)
{
        dist.km <- degrees * 60 * 1.852
        dist.km
}

# this function returns the distance (in km) between two latitudes.
```

```
Positive result means northern travel.
calcDist <- function(lat1, lat2)
{
        diff <- lat2 - lat1
        dist.km <- convertDeg2Km(diff)
        dist.km
}

# combine all output files into one file
source('//Users//kevinsee//Documents//UW_documents//Green Crab//
R Code//plotting_functions.R')
combineOutput <- function()
{
        startLats <- setStartPts()$bayLat
        bays <- setStartPts()$Bay
        distance <- setOffshoreDistances()
        mod.output <- data.frame(startBay=NA, distOffshore=NA,
        distAdvected=NA, dayReleased=NA, latitude=NA, totDevelopTime=NA,
        date=NA, month=NA, yearReleased=NA)
        for(i in 1:length(bays))
        {
                startBay <- bays[i]
                startLat <- startLats[i]
                for(j in 1:length(distance))
                {
                        dist <- distance[j]
                        temp1 <- splitIntoYrs(readOut(dist, startBay))
                # drop all larvae not fully developed
                        temp2 <- temp1[temp1$devPercent == 1,]
                # drop all unimportant columns
                        temp3 <- temp2[,-c(3,4)]
                        distAdvected <- calcDist(startLat, temp3$latitude)
                # add columns for startBay and distOffshore
                        temp4 <- data.frame(startBay=startBay,
                        distOffshore=dist, distAdvected=distAdvected,
                        temp3)

                        mod.output <- rbind(mod.output, temp4)
                }
        }
        mod.output[-1,]
}
```

Running the Model

```
# Set latitudes of possible starting points, in dec deg
StartPts <- data.frame(Bay=c('SF', 'BB', 'HB', 'CB', 'WB', 'GH'),
bayLat = c(37.78, 38.3, 40.75, 43.35, 46.68, 46.9))
# set distance offshore that larvae will drift at
distance <- c(10, 15, 20, 25, 30, 35, 40, 45)
```

```
# run model for consecutive years
for(i in 1:length(distance))
{
        dist <- distance[i]
        # get all velocity data
        velData <- read.table(paste("//Users//kevinsee//Documents//
        UW_documents//Green Crab//Data//ROMS data//Velocity//
        vel_",dist,".xls", sep=''), header=T)

        # get all temperature data
        tempData <- read.table(paste("//Users//kevinsee//Documents//
        UW_documents//Green Crab//Data//ROMS data//Temperature//
        temp_",dist,".xls", sep=''), header=T)

        # run model with larvae starting at each estuary
        nstep <- 784
        for(j in 1:dim(StartPts)[1])
        {
                bayName <- StartPts[j,1]
                bayLat <- StartPts[j,2]
                output <- run.model(velData, tempData, nstep, bayLat)
                # write output to disk
                write.table(output, paste("//Users//kevinsee//Documents//
                UW_documents//Green Crab//R code//OutputFiles//
                ", bayName, "_", dist, ".xls", sep=''), quote=F, sep="t",
                 row.names=F)
        }
}

# combine all output into one large file
allOutput <- combineOutput()
write.table(allOutput, "//Users//kevinsee//Documents//UW_documents//
Green Crab//R code//OutputFiles//allOutput.xls", quote=F, sep="t",
row.names=F)
```